ELSEVIER

Coastal Engineering 47 (2003) 355–365

Coastal Engineering
An International Journal for Coastal, Harbour and Offshore Engineers

www.elsevier.com/locate/coastaleng

Settlement of vertical piles exposed to waves

J. Carreiras[a,1], J. Antunes do Carmo[b,*], F. Seabra-Santos[b,2]

[a] *Polytechnic Institute of Tomar, Estrada da Serra, 2300 Tomar, Portugal*
[b] *IMAR, Department Civil Engineering, Faculty of Science, University of Coimbra, Polo II-Pinhal de Marrocos, 3030-290, Coimbra, Portugal*

Received 30 May 2001; received in revised form 16 September 2002; accepted 11 October 2002

Abstract

In recent years, several authors have conducted experimental studies on the scour around piles fixed in the wave flume. In addition, the settlement of structures has been studied for the case of pipelines, due either to steady currents [International Journal of Offshore and Polar Engineering 4 (1) (1994) 30] or to wave forcing [Coastal Engineering 42 (2001) 313]. However, the settlement of a pile due to scour in waves has so far not been investigated.

This paper reports an experimental study on the settlement of vertical cylindrical piles, either surface-piercing or entirely submerged, exposed to waves.

The primary objective of the study was to investigate: (i) the scour-settlement process with piles of differing heights and densities with their bases initially lying on the seabed and (ii) the influence of the piles height and weight on the hydrodynamics vertical settlement.

A series of experiments was carried out using isolated vertical cylinders of a given diameter (30 mm), different materials (PVC, aluminium, brass, copper and bronze) and different heights (30, 6 and 3 cm). The characteristics of the waves remained constant in all tests (water height = 15 cm, wave period = 2.1 s, local wave height = 4.0 cm, Keulegan–Carpenter number = 12).

The cylinders were set up over a sand bed, so that they could move vertically. Both the initial settlement of each cylinder (when it occurs), due to its weight, and the evolution of additional settlement caused by flow-induced scour were measured. The tests were conducted over a period of 4000 wave cycles.

Keywords: Settlement; Scour; Waves; Cylindrical piles; Laboratory experiments

1. Introduction

As marine structures are often located on erodible bottoms, the scouring action of waves and currents may lead to their damage or failure. In order to avoid these risks, the knowledge of the processes involved in the phenomenon of scour is an essential factor, both for designing coastal structures and for considering preventive measures. A few studies have been conducted in this area, but much more research is still needed. Of particular importance is the study of the mechanisms responsible for scour around cylindrical piles exposed to waves.

Sumer et al. (1992) showed that the generation of lee wake vortices and of a horseshoe vortex at the

* Corresponding author. Tel.: +351-239-797-153.
E-mail addresses: jcarreiras@ipt.pt (J. Carreiras), jsacarmo@dec.uc.pt (J.A. do Carmo), fseabra@ci.uc.pt (F. Seabra-Santos).
[1] Tel.: +351-249-328160.
[2] Tel.: +351-239-797-157.

0378-3839/02/$ - see front matter © 2002 Elsevier Science B.V. All rights reserved.
PII: S0378-3839(02)00142-4

bottom of the pile is responsible for the local scour holes observed in oscillatory flows. For monochromatic waves produced by a wave generator, they found a scaling relationship between the depth of local scour and the Keulegan–Carpenter number, $KC = U_m T/D$ (U_m, T and D designate the amplitude of the wave velocity variations near the bed in the absence of the pile, the wave period and the pile diameter, respectively). It is recognized that this KC number is the major parameter governing local scour processes around cylindrical piles exposed to waves.

According to Carreiras et al. (2000), the KC number may equally be defined as a function of the stroke of the horizontal excursion, $2\hat{a}$, relative to the diameter of the cylinder, D

$$KC = \frac{2\hat{a}}{D}\pi \tag{1}$$

Experiments conducted by Carreiras et al. (2000) on the local scour produced by regular, nonlinear waves around a single pile have shown that in live bed conditions, a good fit is obtained for the equilibrium scour depth, S, and the KC number defined by Eq. (1). The following expression seems to provide a good representation of the scour

$$\frac{S}{D} = 1.3\left[1 - e^{-0.06(KC-6)}\right] \tag{2}$$

Whitehouse (1998) reports that several authors have conducted experimental studies on the scour around piles fixed at the wave flume, in the last few years. However, the settlement of marine structures has only been studied for the case of pipelines, brought about either by steady currents (Sumer and Fredsøe, 1994) or by wave forcing (Sumer et al., 2001).

The primary aim of this study was to investigate the settlement of vertical cylindrical piles, initially lying on the seabed, and to evaluate the influence of their weight and height on scour and vertical settlement in a wave-induced flow. The combined scour and settlement processes were studied, both for surface-piercing piles and for shorter piles entirely submerged in the water. As the settlement due to wave forcing is induced by the scour process around the base of the pile, the settlement measured in the experiments was also compared with the scour predicted by Eq. (2) and measured for fixed piles.

The results of this research may be applied to real marine problems such as: (a) subsea structures that are deployed on the seabed (such as valve stations), (b) structures temporarily deployed on the seabed carrying instruments for field measurements, (c) sinking of armour blocks for scour protection in seabed founded structures.

2. Materials and methods

The experiments were conducted in a wave flume, 0.3 m wide and 7.5 m long, at IMAR (University of Coimbra). The piles were set up over a flat horizontal sand pit, so that they could move vertically (Fig. 1 and Picture 1). The mean sand grain size was $d_{50} = 0.27$ mm. Regular wave conditions were generated. Wave height and ADV velocity were recorded.

A set of experiments was conducted on isolated vertical cylinders of a given diameter (30 mm), made from various materials (PVC, aluminium, brass, copper and bronze) and of different heights (30, 6 and 3 cm). Pile specific gravity, s_p (Table 1), is defined as $s_p = \gamma_{pile}/\gamma_w$, where γ_{pile} and γ_w are the specific weight of the pile and the specific weight of the water, respectively. Some of the pile specific gravities were obtained by combining different materials or, in the case of 30-cm cylinders, by applying additional weight. All the cylinders have hydraulically smooth surfaces.

The initial settlement of each cylinder (when it occurs), caused by its weight, was measured, as well as the evolution of any additional settlement due to

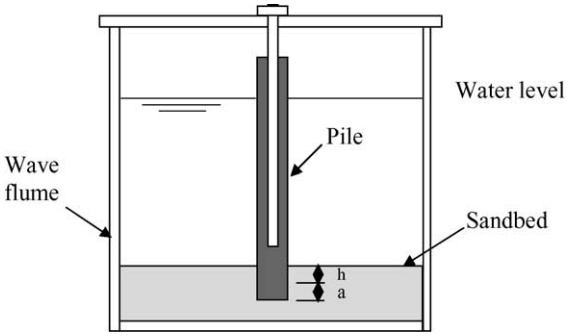

Fig. 1. Experimental set-up.

scour induced by the flow. The accuracy of the measurements was 0.1 mm. All tests were conducted over a period of 4000 wave cycles, a sufficient time to reach the equilibrium scour and settlement depths, according to Herbich et al. (1984) and to our observations.

The characteristics of the waves were constant for all tests. The characteristics of the undisturbed flow at the pile location were: water depth, $h_w = 15$ cm; wave period, $T = 2.1$ s; local wave height, $H_L = 4.0$ cm; amplitude of the wave velocity variations near the bed (average between the crest and the trough measured values), $U_m = 17.2$ cm/s; Keulegan–Carpenter number (calculated by Eq. (1)), KC = 12. Figs. 2 and 3 show the water surface displacement and the horizontal velocity component at the pile location, respectively, in the absence of the pile. The stroke of the horizontal excursion close to the bottom, $2\hat{a} = 11.5$ cm, was computed by integrating the measured local velocity.

The experiments were conducted in live bed conditions. The Shields parameter is defined by

$$\theta = \frac{U_{fm}^2}{g(s-1)d_{50}} \tag{3}$$

in which U_{fm} is the maximum value of the undisturbed bed shear velocity ($U_{fm} = U_m\sqrt{f/2}$, where f is the friction coefficient, calculated for laminar flow in our case), s is the specific gravity of sand grains, d_{50} is the mean sand grain size and g is the acceleration due to gravity. From the flow and sand measured characteristics were obtained, $U_{fm} = 1.7$ cm/s and $\theta = 0.07$ ($\theta > \theta_c$).

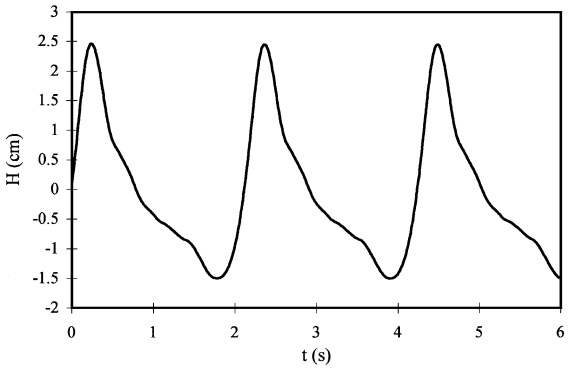

Fig. 2. Wave height record at the pile location.

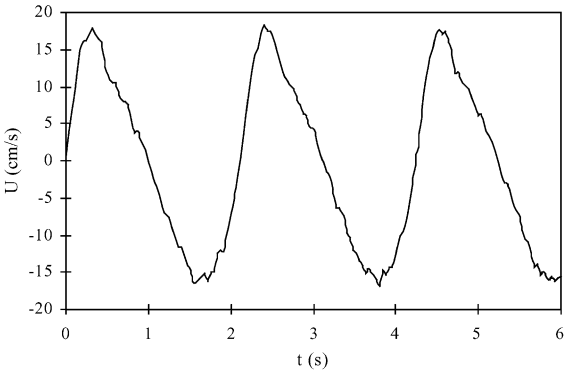

Fig. 3. ADV record at the pile location.

The pile Reynolds number, equal to 5×10^3, was calculated by

$$Re = \frac{U_m D}{\upsilon} \tag{4}$$

where υ is the kinematic viscosity of the water.

3. Theoretical geotechnical background

When a pile is set on the surface of a soil, a settlement occurs below the loaded area. Like most materials, soil has some degree of elasticity, but the load–deformation relationship in soils is relatively nonlinear, even for low ranges of load.

Small bearing stresses correspond to a relatively elastic vertical compression and some lateral distortion of soil under the load. This deformation is primarily attributed to the densification of the stratum as a result of the reduction in voids within the soil mass. In this case, the soil beneath the base of the pile is in a state of elastic equilibrium (Cernica, 1995).

If the load is increased beyond a critical value, the failure of the soil stratum occurs, heavy vertical penetration takes place, and the soil enters into a different state of equilibrium. The critical load required to produce this failure of the soil support is called the total bearing capacity. The average critical load per unit of bearing area is known as the bearing capacity of the soil or the ultimate bearing capacity (Terzaghi, 1943).

The failure of the soil occurs through the sliding of the soil beneath the base of the pile over the failure surface in the two outward directions. Fig. 4 shows the zones developed within the soil stratum with the failure of the soil by plastic flow. The load is transmitted through the soil by the penetrating wedge (zone 1), which is assumed to remain intact during failure, and where the major stresses are vertical. The two zones, 2, of radial stress, throughout which arbitrary failure planes develop, and the two passive Rankine zones, 3, are pushed aside while the pile settles into the bed (Terzaghi, 1943). The soil failure only occurs if the pressure exerted by the load onto the soil adjoining the inclined boundaries of zone 1 is greater than the passive soil pressure (vertical components, Fig. 4). The ultimate bearing capacity is, therefore, calculated under the condition that the sum of the vertical components of the forces that act on the soil volume of zone 1 must be equal to 0.

According to the Terzaghi theory, the formula for estimating the total bearing capacity for general shear failure in the case of cylindrical piles for noncohesive soils is

$$q_u = \gamma' B N_q + 0.3\gamma' D N_\gamma \quad (5)$$

in which q_u is the ultimate bearing capacity ($q_u = Q/A$, where Q is the bearing capacity load in N and A is the bearing area in m^2), γ' is the submerged unit weight of soil in N m^{-3}, B is the depth of the base of the pile in the soil in m, D is the diameter of the pile in m, and N_q and N_γ are the nondimensional bearing capacity factors, whose values depend only on the value of the angle of internal friction of sand, ϕ (Terzaghi, 1943).

In Eq. (5), the first term is the surcharge that represents the effects of the weight of the soil above the level of the base of the pile and is equal to 0 when the pile lies over the surface of the soil. The second term is given by computing the weight of the soil located over the sliding surface (zones 2 and 3 in Fig. 4).

The submerged unit weight of soil, γ', is calculated by

$$\gamma' = \gamma_{sat} - \gamma_w \quad (6)$$

where γ_{sat} is the saturated unit weight that may be obtained by

$$\gamma_{sat} = \frac{(s+e)}{1+e}\gamma_w \quad (7)$$

in which s is the specific gravity of soil solids and e is the void ratio (ratio between the volume of voids and the volume of solids).

The properties of the sand used in the experiments were determined in laboratory measurements and were as follows: mean sand grain size, $d_{50} = 0.27$ mm; void ratio, $e = 0.67$ and angle of internal friction, $\phi = 41°$. With these values, and assuming that the specific gravity of sand grains is $s = 2.65$, $\gamma_w = 9810$ N m^{-3}, $\gamma' = 9700$ N m^{-3}, $N_q = 94$ and $N_\gamma = 123$ were obtained (Bowles, 1968; Cernica, 1995).

In this study, as the piles were founded over the sand bed, the first term of Eq. (5) is initially equal to 0 and the ultimate bearing capacity calculated by this formula is $q_u = 10.7$ kPa, which is the critical bearing stress above which significant initial settlement would be expected.

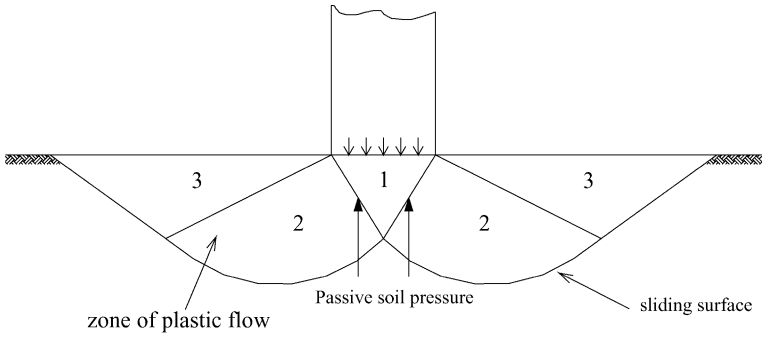

Fig. 4. Definition sketch of general shear failure.

If the bearing stress due to the pile weight exceeds the ultimate bearing capacity and plastic deformation of the sand bed occurs, the pile moves downwards until a new equilibrium of forces is reached, as previously described. The surcharge due to the weight of the soil above the sliding surface is very important in this new equilibrium and is expressed by the first term of Eq. (5).

4. Results and discussion

Table 1 gives the experimental data obtained in this work. The series of 22 experiments may be divided in two groups: the tests with the 30-cm piles (1–10) and the tests with the shorter 6- and 3-cm piles (11–22). As the mean water depth was 15 cm, the 30-cm piles were surface-piercing, and the 3- and 6-cm piles were always entirely submerged. The pressure over the sand bed was calculated as the difference between the pile weight and the buoyancy per unit of area for the surface-piercing piles and as the submerged pile weight per unit of area for the shorter piles.

Table 1
Experimental data

Experiment	Pipe height (cm)	Specific gravity	Pressure over seabed (Pa)	Settlement		Expected scour (Eq. (2))
				Initial h/D	Additional a/D	
1	30	2.4	5684	0.03	0.43	0.39
2	30	7.5	20 711	0.37	0.45	0.39
3	30	5.7	15 437	0.25	0.41	0.39
4	30	4.1	10 460	0.04	0.41	0.39
5	30	8.0	22 167	0.28	0.39	0.39
6	30	1.3	2216	0.03	0.33	0.39
7	30	0.7	735	0.00	0.39	0.39
8	30	8.0	22 128	0.31	0.36	0.39
9	30	8.9	24 782	0.32	0.41	0.39
10	30	11.6	32 773	0.48	0.35	0.39
11	6	2.7	1003	[a]	0.19	–
12	6	8.9	4666	[a]	0.26	–
13	6	6.5	3228	[a]	0.28	–
14	6	4.6	2120	[a]	0.21	–
15	6	8.9	4646	[a]	0.20	–
16	6	1.4	247	[a]	0.17	–
17	3	2.7	503	[a]	0.16	–
18	3	8.9	2336	[a]	0.17	–
19	3	6.6	1638	[a]	0.20	–
20	3	4.6	1072	[a]	0.19	–
21	3	9.0	2347	[a]	0.19	–
22	3	1.4	123	[a]	0.17	–

[a] Values not measured.

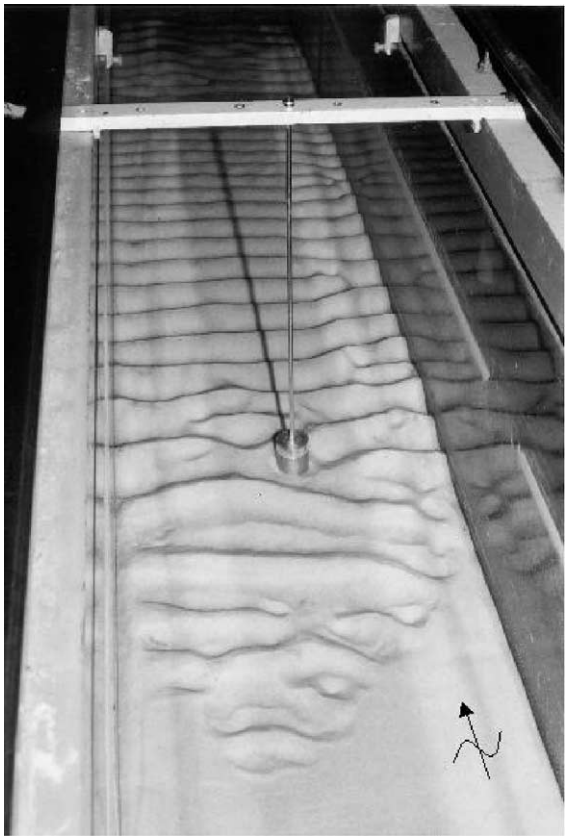

Picture 1. General view of experiment 20.

Picture 1 shows a general view in the onshore/offshore direction and the details of experiment 20.

4.1. Initial settlement

In the experiments with the surface-piercing piles, an initial settlement occurs before the flow is established, caused simply by the action of the pile's weight. This initial settlement is not significant when the pressure over the bottom is less than 10.7 kPa, which agrees with the ultimate bearing capacity obtained in Section 3 by the Terzaghi theory. At this point, it increases steadily with the pressure, as shown in Fig. 5, which gives the plots for the nondimensional initial settlement, h/D, ver-

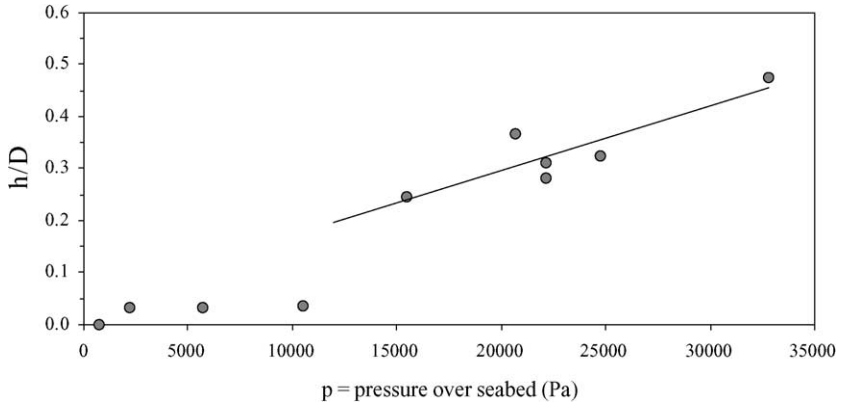

Fig. 5. Initial settlement for the surface-piercing piles.

sus the pressure over the seabed. Therefore, in the cases in which the load exceeds the bearing capacity of the soil, an important initial settlement occurs until a new state of equilibrium is reached, as described in Section 3.

In the tests with the shorter piles, the initial settlement is always very small (< 1 mm). Both for practical reasons and also because its values are not significant for this study, initial settlement was not considered in the 6- and 3-cm-pile experiments.

4.2. Hydrodynamics induced settlement

An oscillatory flow around the base of a vertical cylinder consists of two basic structures: the horseshoe vortex, developed in the boundary layer on the bed, at the front, because of the rotation in the incoming flow velocity, and the lee wake vortices, caused by the separation of the boundary layer over the cylinder surface. The action of this vortex system governs the scour around the pile, as shown by Sumer et al. (1992).

The Reynolds number of the undisturbed wave boundary layer, Re_w, can be defined by

$$Re_w = \frac{\hat{a}U_m}{\upsilon} \tag{8}$$

where $\hat{a}$ is the amplitude of the undisturbed oscillatory flow.

As the oscillatory flow corresponding to our experiments is laminar ($Re_w = 10^4$, by Eq. (8)), the thickness of the undisturbed wave boundary layer is $\delta = 0.2$ cm, obtained by the following equation (Sumer et al., 1997):

$$\frac{\delta}{\hat{a}} = \frac{3\pi}{4}\left(\frac{2}{Re_w}\right)^{1/2} \tag{9}$$

In both groups of experiments (surface-piercing piles and shorter piles), the horseshoe vortex is generated at the bottom of the cylinder, and the erosion caused by vortex-shedding, around the pile, produce sediment transport and erosion as well as the formation and propagation of ripples. These scour processes developed slowly in the tests with the shorter cylinders.

The visualization of the scour processes in the experiments with the 30-cm piles showed two different scenarios. When the pressure over the bed and the initial settlement are both small, the sediment erosion around the base of the pile caused by the horseshoe vortex action leads to the formation of a scour hole that extends under the base of the pile. Initially, this process facilitates the settlement of the pile, which depends on the development of the scour hole, and increases rapidly. When the pile penetrates the sand, to a depth sufficient to impede the action of the vortices under the base, settlement stops. In this scour-settlement process, the bearing area is continuously reduced as the scour extends under the pile. Then, the bearing stresses increase continuously, which induces successive settlements and new states of equilibrium in the soil until an equilibrium scour depth is reached. Similar findings were reported by

Sumer et al. (2001) for the sinking of pipelines under waves.

On the other hand, when very high pressure over the bed causes considerable initial settlement, the scour processes induce an additional settlement. The rate of this process depends on the depth of the scour hole around the pile. In this case, the bearing capacity of the soil has been exceeded initially, as described in Section 3. After the flow begins, the vortices generated around the pile continue to remove an amount of sediment during the course of the scour process. Therefore, the weight of the soil above the failure surface (first term of Eq. (5)) and the passive soil pressure acting over the inclined boundaries of zone 1 (Fig. 4) both decrease. The bearing capacity of the soil is then lessened and the equilibrium in the soil is continuously broken. As a consequence, a succession of settlements and states of equilibrium occur. The scour-settlement process is more progressive in this case, and settlement equilibrium depth is reached slowly.

Fig. 6 shows the time series of the nondimensional settlement (a/D, where a is the additional settlement and D is the pile diameter) for some representative experiments. In tests 6 and 7, where the pile weight is small, 90% of the settlement depth is reached in 900 wave periods. In the tests that correspond to the highest pressure over the seabed (9 and 10), the same amount (90%) of the settlement depth is reached in 1300–1700 wave periods.

In the tests with the shorter cylinders, namely, in experiment 14 (also represented in Fig. 6), the pressure over the bed is low and no initial settlement occurs. The hole formed around the pile by the scouring action of the vortices thus initially extends under the base of the piles. Moreover, the settlement reaches the equilibrium depth rapidly.

The experimental data given in Table 1 is also represented in Figs. 7 and 8, in which H represents the cylinder height.

The additional or hydrodynamic-induced settlements are shown in Fig. 7 for all experiments. In the tests with 30-cm piles, the additional settlement is virtually constant and has a value significantly close to the expected scour depth, given by the scaling relationship between the depth of local scour and the Keulegan–Carpenter number. This is demonstrated in Fig. 7, which shows the plots of the linear regression line that fits the group of data corresponding to the surface-piercing piles and the straight line corresponding to the expected equilibrium scour depth, S/D, calculated by Eq. (2). These two lines practically coincide. Scour, therefore, appears to be the key element in the process of pile settlement. In spite of the different characteristics of the scour-settlement process, significant initial settlement, as described

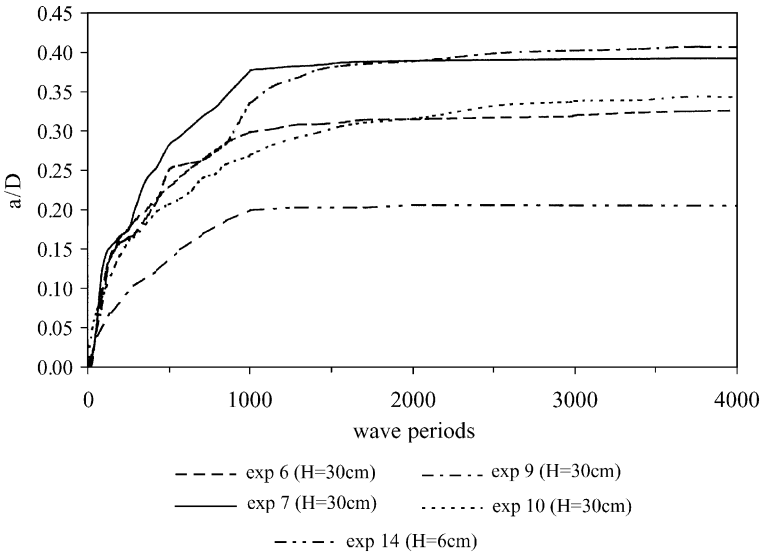

Fig. 6. Time series of additional settlement.

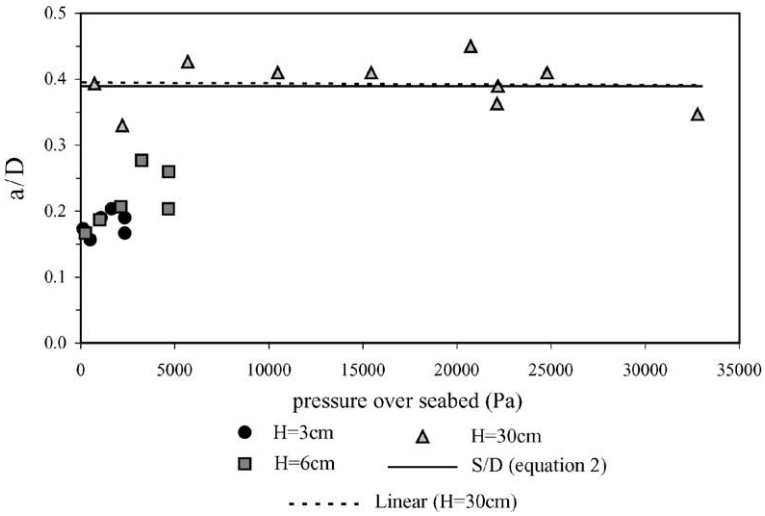

Fig. 7. Additional settlement versus pressure over seabed after 4000 waves.

above, may or may not occur, and this process always develops as seeing the initial settlement depth as the initial seabed level.

However, values obtained for shorter cylinders are lower for pressures of the same magnitude, as shown in Fig. 7, and in Fig. 8, which is basically a close-up of the previous one. Fig. 8 displays the experimental data for the tests with the 6- and 3-cm piles and also the linear regression lines corresponding to these two groups of data. In these cases, the settlement increases slightly with pressure, but is virtually independent of the height of the pile.

The thickness of the wave boundary layer, calculated by Eq. (9), suggests that the horseshoe vortex is not significantly altered by a reduction of pile height and is, therefore, not responsible for the difference in the magnitude of the settlements. In fact, the horseshoe vortex is formed in the boundary layer, whose thickness is much less than the piles' height, even in the case of the shorter ones. On the other hand, the downstream vortex shedding that results from the interaction between the two shear layers issuing from the side edges of the pile (Sumer et al., 1992) and the vertical downflow produced at the exposed face of the

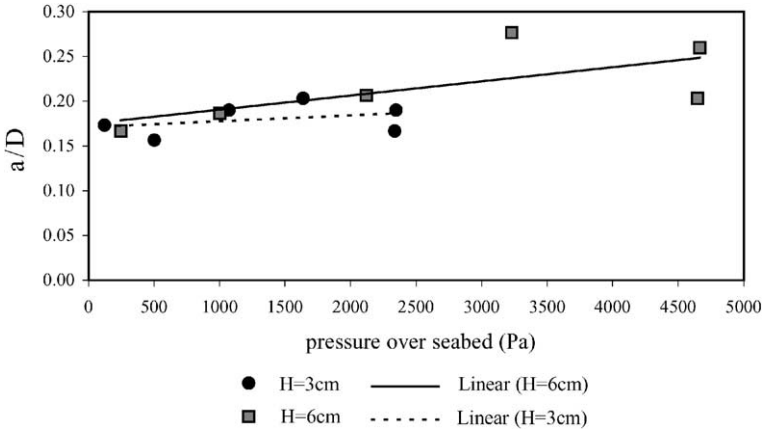

Fig. 8. Additional settlement versus pressure after 4000 waves (6- and 3-cm piles).

Table 2
Experiments with fixed piles

Experiment	D (mm)	KC	H (cm)	S/D
1	30	12	3	0.20
2	30	12	6	0.26
3	30	12	30	0.40

cylinder, in each period, might be influenced by the pile height. This may induce a change in the three-dimensional effect of the turbulence around the base of the shorter piles, which could inhibit scour and settlement.

To investigate the influence of the pile height on scour, a complementary series of three experiments with fixed piles was conducted (Table 2).

Flow visualization shows that the vortices and the sediment transport are much more important in the surface-piercing pile than in the shorter piles, especially in the 3-cm pile. On the other hand, a quasi-equilibrium scour configuration is reached rapidly with the shorter piles, while the evolution until equilibrium is slower in the 30-cm-pile experiment.

The depths obtained for the equilibrium scour, in the three cases, are of the same order of magnitude as the settlements obtained for movable piles of the same height. As ripples in the live bed case induce slight variation over an equilibrium configuration in the scour hole (see Section 4.4), the equilibrium scour depth is assumed to be the depth, over which these little variations take place, measured close to the pile. The findings appear to confirm that scour is the key element governing the settlement of piles in waves.

4.3. Time scale of settlement process

The evolution of the hydrodynamics induced pile settlement towards the equilibrium stage was described for the different cases in Section 4.2. The time series of some representative experiments are plotted in Fig. 6. The time scale of the process may be defined by the following equation (Sumer et al., 2001):

$$T_s = \frac{1}{a}\int_0^{\infty}(a - a_t)\mathrm{d}t \qquad (10)$$

in which a is the equilibrium additional settlement and a_t is the additional settlement at time t.

The time scale represents the time over which a significant amount of settlement takes place. As the sediment characteristics are invariable in all the experiments, the time scale may be normalized with the wave period in order to obtain $T^* = T_s/T$, expressing the time scale in a number of wave periods. Fig. 9 gives the plot for the time scale, T^*, as a function of the nondimensional additional settlement, a/D. The data is divided in two groups: the first is formed by the experiments in which the pressure over the bed is lower than the bearing capacity of the soil, and the second corresponds to the experiments in which significant initial settlement was observed.

According to the above description of the different settlement processes, the time scale is smaller when the pressure over the bed and the initial settlement have lower values (the two lower values of $p < q_u$ in Fig. 9). This is because the scour induced by the flow extends rapidly under the pile and facilitates a faster settlement into the bed, as explained before. In the four cases group where the initial settlement is not significant ($p < q_u$), the time scale increases with a/D. Really, as the pile weight increases, the scouring action of the vortices extends under the base of the pile between successive settlements by a smaller area. The pile settles, step by step, in a more progressive and gradual way than in the previous experiments.

When initial settlements are caused by bearing stresses greater than the ultimate bearing capacity ($p < q_u$), and failure of the soil occurs, the time scale is almost nonvariable and tends to a maximum value, as shown in Fig. 9. This is because the vortex system

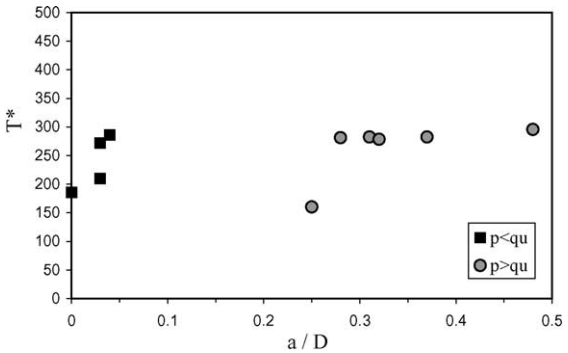

Fig. 9. Time scale of settlement process.

in these tests does not act under the base of the pile, and the scour-settlement process is similar in all the cases, resulting only from the removal of soil particles around the pile. This process is described in the previous section. One of these tests had a nonexpected behavior (a too small value of T^*), which we believe is not relevant to our conclusions.

4.4. Scale effects

The pile Reynolds number, the surface roughness of the pile, the Shields parameter and the presence of wave-induced ripples may produce scale effects in small-scale laboratory experiments.

The Reynolds number, together with the surface roughness of the pile, influences the downstream flow, namely, the vortex shedding pattern. However, Sumer et al. (1992) found that this influence is not significant to the equilibrium scour depth, at least for the Re_w number range of these experiments. The same authors also showed that the variation of the scour depth with θ is weak in the case of live bed conditions. It may thus be expected that the effects due to these three parameters are insignificant in the scour-settlement process.

In all the experiments, ripples were generated by the oscillatory flow. The ripple length is about 5 cm and the ripple height has the same order of magnitude as the scour, which was measured relative to the initial plane bed. Sumer et al. (1992) and Sumer and Fredsøe (1994) argue that the ripple effect is small, because ripples are not present in the immediate neighborhood of the pile, where the disturbed flow field inhibits ripple formation. However, ripple dynamics does cause a periodic fluctuation over the equilibrium scour depth around the pile. Indeed, in the presence of ripples, the equilibrium scour around a pile, in nonlinear waves, does not have an ultimate configuration, but changes, albeit not significantly, with the ripple motion in the neighborhood of the scour hole.

5. Conclusions

The settlement of piles exposed to waves, either surface-piercing or entirely submerged in water, was investigated. Depending on the pile's weight, an initial settlement may occur before the flow is established. The main conclusions of this study are as follows:

(i) The initial settlement is only significant when the pressure over the bottom exceeds the bearing capacity of the soil, after which it seems to increase steadily with the pressure.
(ii) The additional settlement is virtually constant for the surface-piercing piles and has a value significantly close to the expected scour depth predicted by the scaling relationship between the depth of local scour and the Keulegan–Carpenter number (Carreiras et al., 2000).
(iii) For shorter cylinders, the values obtained are lower, but even in these cases, the settlement does not increase significantly with pressure and is of the same order of magnitude as the scour depth found for fixed piles.
(iv) Scour appears to be the key element in the piles' hydrodynamics-induced settlement, and the scour-settlement process is influenced by the pile's height.

Further investigation into the settlement of piles on a sand bed is needed and is planned by the authors. An experimental study using different soils and KC numbers, corresponding to a variety of hydrodynamic conditions and/or different pile diameters, and the establishment of design diagrams of the expected pile settlement as function of KC is a priority.

List of symbols

A	Bearing area
a	Additional settlement of the pile
a_t	Additional settlement at time t
$\hat{a}$	Amplitude of the undisturbed oscillatory flow
B	Depth of the base of the pile
D	Pile diameter
d_{50}	Mean sand grain size
e	Void ratio
f	Friction coefficient
g	Acceleration due to gravity
H	Pile height
H_L	Wave height
h	Initial settlement of the pile
h_w	Mean water depth
KC	Keulegan–Carpenter number

N_q, N_γ	Bearing capacity factors
n	Porosity of sand
Q	Bearing capacity load
q	Bearing capacity of the soil
Re	Pile Reynolds number
Re_w	Reynolds number of the undisturbed wave boundary layer
S	Equilibrium scour depth
s	Specific gravity of sand grains
s_p	Pile specific gravity
T	Wave period
T_s	Time scale
T^*	Normalized time scale
t	Time
U_m	Amplitude of the wave velocity variations near the bed
U_{fm}	Maximum value of the undisturbed bed shear velocity
γ_{pile}	Specific weight of the pile
γ_{sat}	Saturated unit weight of soil
γ_w	Specific weight of water
γ'	Submerged unit weight of soil
δ	Thickness of the undisturbed boundary layer
θ	Shields parameter
υ	Kinematic viscosity of water
ϕ	Angle of internal friction of sand

Acknowledgements

This work was undertaken as part of the MAST-3 SCARCOST Program. It has been funded in part by the Commission of the European Communities, Directorate General for Science, Research and Development, under contract MAS3-CT97-0097. The authors would like to thank the reviewers for their comments and suggestions.

References

Bowles, J.E., 1968. Foundation Analysis and Design. McGraw-Hill, USA.

Carreiras, J., Larroudé, P., Santos, F.S., Mory, M., 2000. Wave scour around pilesProceedings 27th International Conference on Coastal Engineering, Sydney, vol. 2. ASCE, New York, pp. 1860–1870.

Cernica, J., 1995. Geotechnical Engineering: Soil Mechanics. Wiley, New York.

Herbich, J.B., Schiller, R.E., Watanabe, R.K., Dunlap, W.A., 1984. Seafloor scour: design guidelines for ocean founded structures. Ocean Engineering, vol. 4. Marcel Dekker, New York.

Sumer, B.M., Fredsøe, J., 1994. Self-burial of pipelines at span shoulders. International Journal of Offshore and Polar Engineering 4 (1), 30–35.

Sumer, B.M., Fredsøe, J., Christiansen, N., 1992. Scour around vertical piles in waves. ASCE Journal of Waterway, Port, Coastal and Ocean Engineering 118 (1), 15–31.

Sumer, B.M., Christiansen, N., Fredsøe, J., 1997. The horseshoe vortex and vortex shedding around a vertical wall-mounted cylinder exposed to waves. Journal of Fluid Mechanics 332, 41–70.

Sumer, B.M., Truelsen, C., Sichmann, T., Fredsøe, J., 2001. Onset of scour below pipelines and self-burial. Coastal Engineering 42, 313–335.

Terzaghi, K., 1943. Theoretical Soil Mechanics. Wiley, New York.

Whitehouse, R., 1998. Scour at Marine Structures. Thomas Telford, London.